CHAPTER FOUR

SYNTHESIS OF CdSe NANOPARTICLES AND PVP, L-CYSTEINE-CAPPED Au-CdSe HYBRID NANOPARTICLES

4.0 INTRODUCTION

The anisotropic growth of nanomaterials has led to the development of complex and diverse nanostructures such as rods [1,2], tetrapods [3], prisms [4], cubes [5], and other non-spherical morphologies [6,7]. The synthesis of metal nanoparticles and that of semiconductors have been widely reported in the literature. Semiconductor particles exhibit size dependent properties such as the scaling of the energy gap and corresponding change in the optical properties. They are considered as the front runners in technologically important materials. CdSe is one of such materials, it shows strong fluorescence which can be tuned according to the particle size. CdSe has been considered in many applications such as optoelectronic devices [8], light sensors [9], biological labels [10], chemical libraries [11] etc.

Nanosized metal chalcogenides particles are important dispersed phases within polymer matrices owing to their important non-linear optical properties, luminescent properties, quantum size effects, and other important physical and chemical properties [12,13]. Such novel properties of the quantum dots (QDs) are generally known as a result of the size quantization of semiconductor QDs and the large surface to volume ratio when compared to bulk materials [14]. Most importantly, CdSe semiconductor has often been investigated due to its well-known physical properties and potentially controllable band-gap energy in the full visible spectral range [15]. CdSe QDs have been synthesized mainly by using organometallic precursors in standard air-less conditions at relatively high temperatures (250 – 500 °C) [16]. However, a few studies investigated the preparation of CdSe QDs at mild conditions at around room temperature [17]. Yu *et al.* prepared highly monodispersed CdS nanocrystals by size-selective photocorrosion [18], while Zhou *et al.* developed an *in situ* ultraviolet irradiation polymerization-photolysis technique for fabrication of polyacrylamide-MS (M = Cd, Pb, and Zn) nanocomposites at room temperature [19]. Most classical preparative and spectroscopic studies have been carried out on CdSe nanocrystal with hexagonal (wurtzite) structures. These were obtained by the reaction of cadmium and selenium precursors in the presence of the stabilizing agents tri-*n*-octylphosphine oxide (TOPO), trioctylphosphine (TOP) and

hexadecylamine (HAD) at high temperatures [20,21]. CdSe nanocrystals with a cubic (zinc-blende) structure have been synthesized by several groups [22,23].

The synthesis of multi-component materials comprising of a metal and semiconductor material have also been developed. This combination provides new functionalities to the nanostructures. Systems like these represent a new class of materials, where catalytic metals are paired with a semiconductor material within the same structure. These heterostructured materials have been studied as photocatalysts in photochemical water splitting to produce hydrogen in photoelectrochemical cells, and in photochemical purification of organic contaminants, and bacterial de-toxification [24]. The excitation of the surface plasmon in metal nanoparticles placed into a semiconductor can be expected to enhance optical phenomena, such as absorption and photoluminescence of incident photons within the semiconductor region near each nanoparticle due to localized field amplification. Saunders *et al.* have reported a novel route to form heterostructures by the selective growth of metals on semiconductors [25]. Numerous approaches have been used to selectively grow metals on semiconductors such as reduction, physical deposition or photochemical methods. Au-CdSe [26], Au-CdS [25], Au or Ag on ZnO [27], Co and Au on TiO_2 [28] are examples of hybrid nanoparticles that have been developed. Pullabhotla and Revaprasadu [29] have synthesized Au-CdSe hybrid nanoparticles by the reduction of $HAuCl_4$ and selenium powder together with the $NaBH_4$ solution and capping agent.

The main major challenge in synthesizing multicomponent nanostructures is the understanding of how to form an interface between materials which may have different crystallographic structures, lattice dimensions, thermal stability as well as chemical reactivity. The use of these materials then requires identifying and understanding the emergence of new properties due to the combination of different material systems on the nanometer length scale. The optical properties of these nanostructures, often exhibit interesting deviations from either their individual components or from a physical mixture of the two components. These optical effects include a shift in the surface plasmon resonance (SPR) of noble metal nanocrystals when combined or coated with other materials or changes in the photoluminescence intensity of semiconductor nanocrystals

which can be attributed to the overlap of the electronic structures of different components [25,30]. In this chapter the selective growth of two different material systems, that is, a metal onto a semiconductor (Au-CdSe), AuNPs and CdSe nanoparticles is reported. We have recently reported the synthesis of anisotropic gold nanoparticles in water-soluble PVP as a stabilizer using UV-irradiation technique [31], as reported in the previous chapter [Chapter three]. The concentrations of starting materials, lamp wavelength and irradiation time they all played major roles towards determining the size and morphology of the final gold nanoparticles. Our group has reported the synthesis of water-soluble CdSe nanoparticles passivated with cysteine [32]. In current work, the above synthetic procedures were adapted in order to synthesize Au-CdSe hybrid particles.

4.1 EXPERIMENTAL

4.1.1 Materials and Instrumentation

Cadmium chloride, cadmium carbonate, chloroauric acid ($HAuCl_4$), sodium borohydride, acetone, methanol, L-cysteine, tri-octylphosphine, hexadecylamine, polyvinyl alcohol and poly vinyl pyrrolidone were all purchased from Aldrich and selenium powder from Merck. All the chemicals were of analytical grade and used as purchased.

This is explained in Chapter Two under Experimental section.

4.1.2 Synthesis of PVP-Capped CdSe Nanoparticles

In this reaction, selenium powder (0.0253 g, 0.320 mmol) was dissolved in distilled water (20.0 mL) in a three necked round bottom flask under a nitrogen atmosphere. The selenium was reduced by the addition of a solution (20.0 mL) of sodium borohydride (0.030 g, 0.320 mmol). The reaction was allowed to proceed for 3 h in order to allow the complete reduction of selenium. After 3 h a solution (20.0 mL) of $CdCl_2$ (0.0644 g, 0.320 mmol) was simultaneously added with a solution (20.0 mL) of PVP (1.288 g). The Se: Cd: $NaBH_4$: PVP mole ratio of 1:1:1:20 was maintained in this experiment. A further number of reactions were carried out in which different mole ratios were used and cadmium source was changed to a carbonate salt. These mole ratios are outlined in Table 4.1 below.

Table 4.1: Mole ratios used for the synthesis of CdSe semiconductor nanoparticles.

Experiment	Cadmium Salt		Se, mol	$NaBH_4$, mol	PVP, mol
	$CdCl_2$, mol	$CdCO_3$, mol			
1	1	—	1	1	20
2	1	—	1	1	10
3	2	—	1	1	10
4	1	—	2	1	10
5	1	—	1	1	40
6	2	—	1	1	40
7	1	—	2	1	40
8	—	1	1	1	20
9	—	1	1	1	10
10	—	2	1	1	10
11	—	1	2	1	10
12	—	1	1	1	40
13	—	2	1	1	40
14	—	1	2	1	40

4.1.3 Synthesis of PVP-Capped Au-CdSe Hybrid Nanoparticles

In this method, two solutions were prepared at different reaction conditions before they were both mixed in different concentrations in order to produce Au-CdSe hybrid nanoparticles. Firstly, the metal nanoparticles were prepared with the method previously reported [31]. Briefly, in this typical procedure, chloroauric acid (0.3146 g, 4.00 x 10^{-3} M) was mixed with PVP (0.900 g) in distilled water (200.0 mL). This solution was irradiated with UV-light [mercury lamp (450 - 500 nm)] for an hour in order to reduce the metal to form the metal nanoparticles. The CdSe nanoparticles were prepared by dissolving selenium powder (0.0253 g, 0.320 mmol) in distilled water (20.0 mL) in a three necked flask under N_2 atmosphere with continuous stirring. To this solution $NaBH_4$ (0.03 g, 0.320 mmol) dissolved in distilled water (20.0 mL) was added. The $NaBH_4$ was allowed to completely reduce the selenium for 3 h. Cadmium chloride (0.0644 g, 0.320 mmol), dissolved in distilled water (20.0 mL) was then added to this solution to produce CdSe.

To the solution containing CdSe nanoparticles, a solution containing Au-metal nanoparticles (4.00 x 10^{-3} M) was added in order to produce Au-CdSe hybrid particles. This addition resulted in a colour change to purple-wine-red solution. This solution was allowed to completely react for an hour under N_2 atmosphere with continuous stirring.

4.1.4 Synthesis of L-Cysteine-Capped Au-CdSe Hybrid Nanoparticles

In this procedure, an AuNP stock solution and CdSe nanoparticles capped with cysteine were prepared separately. The final step was to mix the two solutions at different concentrations in order to produce Au-CdSe hybrid nanoparticles. The Au-metal nanoparticles were prepared using the UV-irradiation technique discussed in Chapter three. In preparing the metal nanoparticles a mole ratio of $HAuCl_4 \cdot 3H_2O$: L-cysteine (1:40) was used. Briefly, in this typical procedure, chloroauric acid (0.1258 g, 1.60 x 10^{-3} M) was mixed with L-cysteine (1.5508 g, 12.8 mmol) in distilled water (200.0 mL). This solution was irradiated with UV-radiation for an hour in order to reduce the metal

forming L-cysteine capped Au nanoparticles. CdSe nanoparticles were prepared by dissolving selenium powder (0.0253 g, 0.32 mmol) in 20.0 mL distilled water in a three necked flask under N_2 atmosphere with continuous stirring. To this solution $NaBH_4$ (0.03 g, 0.32 mmol) dissolved in distilled water (20.0 mL) was added. $NaBH_4$ was allowed to completely reduce the selenium for 3 h. Then, cadmium carbonate (0.0556 g, 0.32 mmol) dissolved in distilled water (20.0 mL) and cysteine (0.7754 g) (1:20 mole ratio) dissolved in distilled water (20.0 mL) were simultaneously added to this solution resulting in a light brown colour change in the solution, and its intensity increased with the reaction time.

Finally, to the solution containing CdSe nanoparticles a solution containing metal (Au) nanoparticles (1.60×10^{-3} M) was added to produce Au-CdSe hybrid particles. This addition resulted in a colour change to purple-wine-red solution. This solution was allowed to completely react for an hour under N_2 atmosphere with continuous stirring. The solution was finally separated through centrifugation before further analyses were performed. Further experiments were conducted in which different concentrations of metal nanoparticles were added, that is 4.80×10^{-4} M; 3.20×10^{-4} M and 1.60×10^{-4} M respectively.

4.1.5 Synthesis of L-Cysteine Capped Gold Nanoparticles

The gold nanoparticles were synthesized by UV-light through the reduction of $HAuCl_4$ dissolved in distilled water in the presence of L-cysteine. In a typical reaction, $HAuCl_4 \cdot 3H_2O$ (0.1258 g) and L-cysteine (1.5508 g) were both dissolved in distilled water (200 mL) forming a yellow solution. This solution was irradiated with a column like mercury lamp (450 – 500 nm) under nitrogen atmosphere with continuous stirring.

4.1.6 Synthesis of L-Cysteine-Capped Au-CdSe Hybrid Nanoparticles in the UV-Reactor

The synthesis carried in this experiment was nearly the same as above, with differences outlined in the procedure below. Basically, selenium powder (0.0253 g) was

dissolved in distilled water (20.0 mL). This was then reduced by a solution of $NaBH_4$ (0.03g, 20.0 mL). Selenium reduction was allowed to proceed for 3 h to allow its complete reduction. In the UV-irradiation reactor set up, $HAuCl_4 \cdot 3H_2O$ (0.1258 g) and L-cysteine (0.7754 g) dissolved in distilled water were prepared. The reduced selenium and $CdCO_3$ (0.0550 g) solution in distilled water were simultaneously added to the solution in the UV-reactor. The volume of the final solution in the reactor was then increased to 200.0 mL using distilled water.

Finally the UV-reactor reduction with a low-mercury lamp light (450 – 500 nm) was started with all the reactants in one reactor. Initially the solution colour changed from light yellow to brown and then to dark purple colour after 1 h of irradiation. This reaction was repeated three times varying the amount of $HAuCl_4$ added while the other reactants were kept constant, as outlined in Table 4.2.

Table 4.2: Amounts used and varied for the synthesis of L-Cysteine capped Au-CdSe hybrid nanoparticles.

$HAuCl_4$ (M)	**Se (g)**	**$NaBH_4$ (g)**	**$CdCO_3$ (g)**	**L-Cysteine (g)**
1.60×10^{-3}	0.0253	0.0300	0.0550	0.7754
1.20×10^{-3}	0.0253	0.0300	0.0550	0.7754
8.00×10^{-4}	0.0253	0.0300	0.0550	0.7754
4.00×10^{-4}	0.0253	0.0300	0.0550	0.7754

4.2 RESULTS AND DISCUSSION

4.2.1 Synthesis of PVP-Capped CdSe Nanoparticles

CdSe nanoparticles have been synthesized by the reduction of Se powder with $NaBH_4$ in the presence of PVP as the stabilizing agent. Different cadmium sources (carbonate and chloride salts) were used in this study. Various reaction conditions such as cadmium source concentration, selenium concentration, and reducing agents were applied for the controlled synthesis of CdSe QDs as outlined in Table 4.1. The generation of CdSe

nanoparticles could also be identified from both the colour change and the UV-Vis spectra of the as-prepared product. Figure 4.1 presents the UV-Visible absorption spectra of PVP-capped CdSe nanoparticles synthesized using the carbonate salt. The spectra at different mole ratios exhibit weak absorption shoulders at around 300 nm; however, no other features were observed at higher wavelengths. As the mole ratio of the capping agent was increased up to a factor of 4 (from 1:10 to 1:40), smoother curves and longer wavelength shoulders were observed. In order to obtain the structural information and particle morphology of the CdSe nanoparticles, the products were centrifuged before the TEM analysis. Figure 4.2 shows TEM micrographs of the CdSe semiconductor nanocrystals dispersed in the polymer matrix prepared at room temperature at low PVP concentration. Particles with a plate-like morphology were observed. As the PVP concentration was increased i.e. (1:2:10 and 1:2:40) similar plate-like morphologies were observed with the length of the longest plate particle approximately 800 nm.

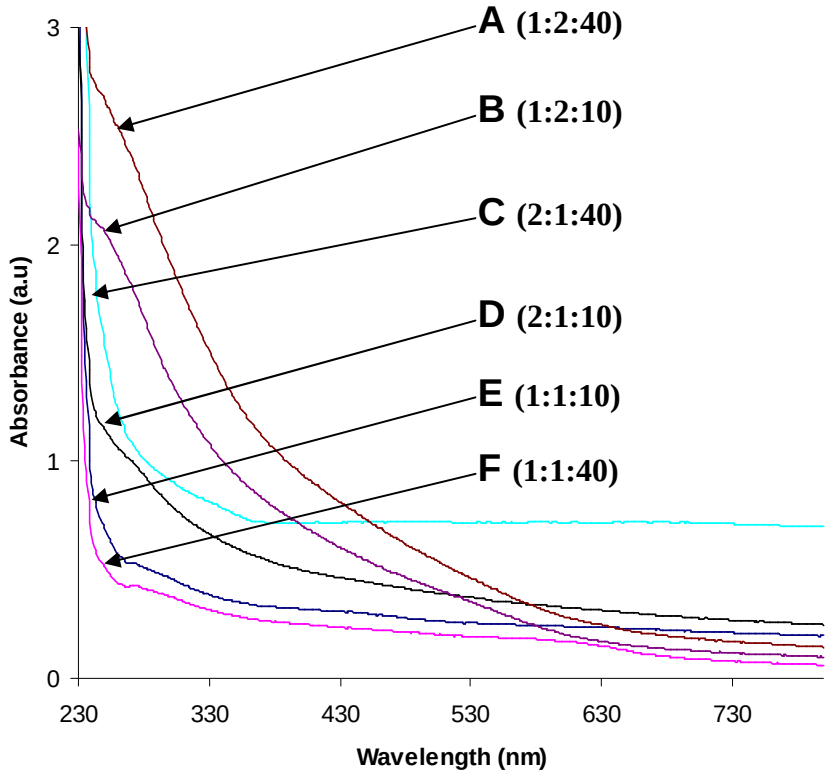

Figure 4.1: *UV-Visible absorption spectra of PVP-capped CdSe semiconductor nanoparticles at different $Cd(CO_3)_2$: Se: PVP ratios: A. (1:2:40), B. (1:2:10), C. (2:1:40), D. (2:1:10), E. (1:1:10) and F. (1:1:40).*

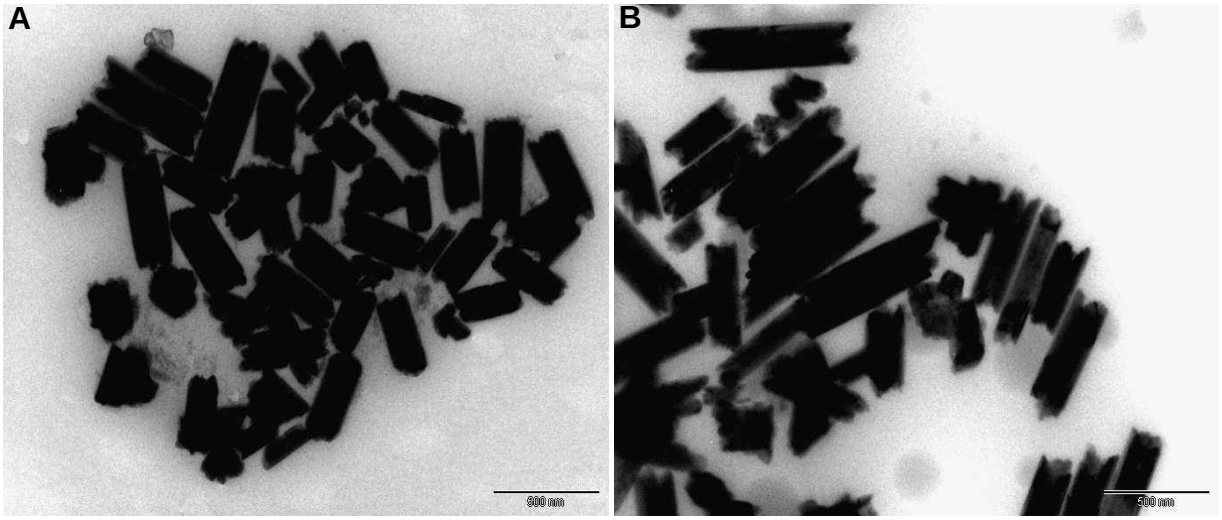

Figure 4.2: *TEM images of PVP-capped CdSe semiconductor nanoparticles at a mole ratio of $Cd(CO_3)_2$: Se: PVP; A. (1:2:10) and B. (1:2:40).*

The shape and the size of gold nanowires depend upon the adsorption of PVP on the surface of the gold particles [33]. The PVP plays an important role in controlling the growth rate between the {100} and {111} plane directions of cubic gold [34]. Reyes-Gasga *et al.* have proposed that nanowires evolve from a multiple twinned nanoparticle (MTP) of silver with the help of PVP at the initial Ostwald ripening stage [35]. The growth of the nanowires was facilitated by PVP selectively covering the {100} facet. This is done through chemical interactions with the nitrogen and or oxygen atoms of the pyrrolidone units of PVP [36]. On the other hand the interaction between PVP and the {111} facet is weaker allowing the nanowires to grow continuously during the Ostwald ripening process. Due to force fields which exist between atoms, they will begin to agglomerate to form colloidal gold particles which are dominated by the {110} facet. The {110} facet forms a weak interaction with the PVP molecules due to the weak binding energy. In the literature it is reported that PVP can bind strongly with the {100} plane as compared to the {111} plane [37]. Since there is competition between {111} and {100} facets to absorb PVP molecules, a certain amount of PVP will be adsorbed on each facet. A concentration of PVP is not favourable for the formation of pentagonal and trigonal shaped particles. The high concentration of PVP leads to the formation of a thick coating over the entire surface of the spherical particles, including the twin boundaries [38].

Powder X-ray diffraction measurements were performed in order to characterize the crystal structure of the CdSe nanocrystals as shown in Figure 4.3. The CdSe displays a polycrystalline hexagonal wurtzite structure. The diffraction pattern of nanocrystals shows (102) and (103) reflections at 2θ = 36.7° and 44.1° respectively, characteristics of the wurtzite phase. The peak around 2θ = 25° in the diffraction pattern of wurtzite CdSe nanocrystals is a combination of (100), (002) and (101) reflections. In agreement with previous studies, the (102) and (103) reflections in the XRD patterns of wurtzite are reduced because of the presence of stacking faults along the (002) direction, a typical phenomenon in wurtzite II-IV nanocrystals [20]. Additional peaks may be due to the impurities in solution.

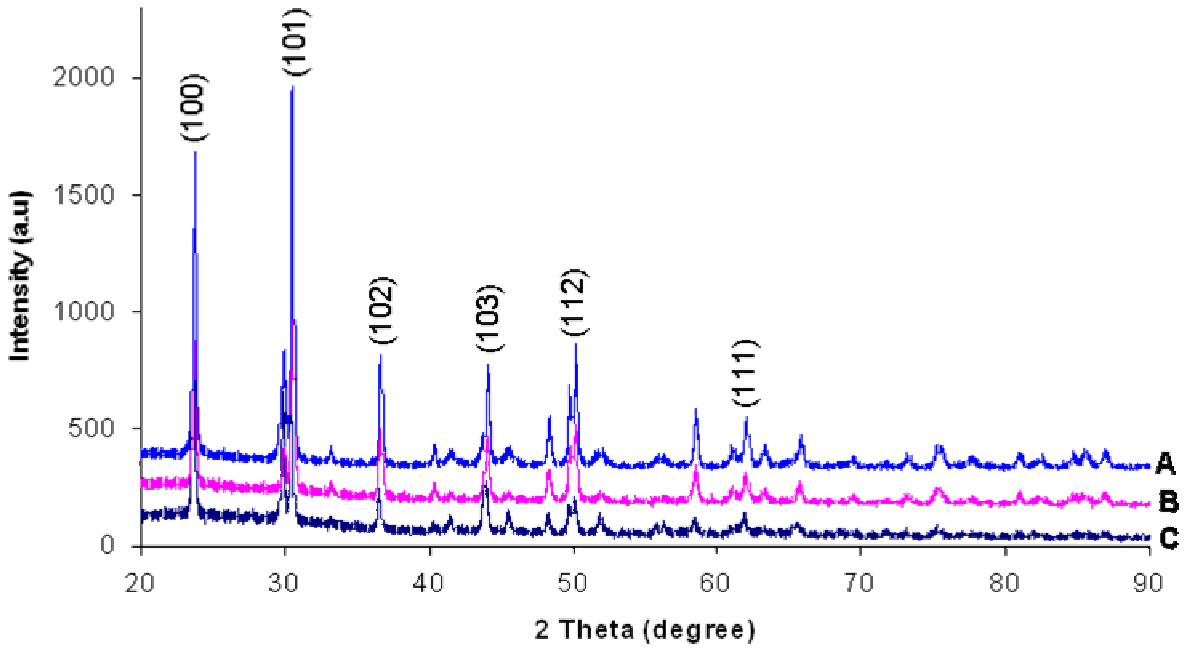

Figure 4.3: *Powder XRD pattern of PVP-capped CdSe semiconductor nanoparticles at different $Cd(CO_3)_2$: Se: PVP ratios: A. (1:1:10), B. (2:1:10), and C. (1:2:40).*

The cadmium source was further changed to a chloride salt with the mole ratios kept constant as outlined in Table 4.1. The optical properties and structural information of the produced CdSe nanoparticles were obtained from the UV-Visible and TEM. Figure 4.4 shows the UV-Visible absorption spectra of these semiconductors dispersed in PVP. The CdSe QDs prepared with chloride salt present the absorption spectra with similar spectral

changes to that of the CdSe QDs prepared with a carbonate salt. Beside the absorption shoulders no peak or distinct band gap in the UV for the CdSe particles are observed. Similar spectral overlap has previously been observed in semiconductor QDs with multiple size distribution [39].

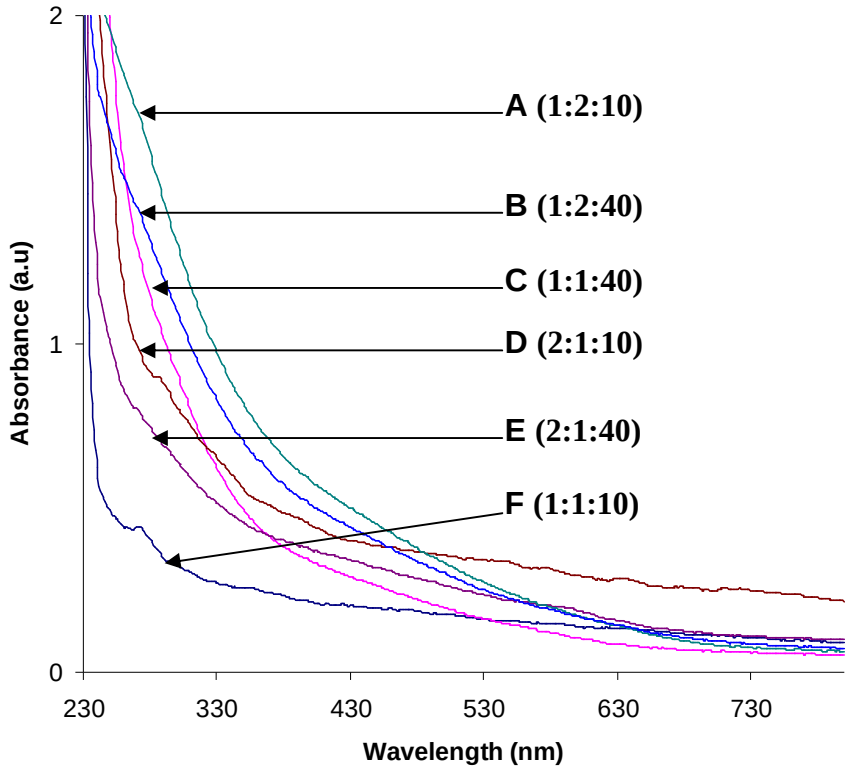

Figure 4.4: *UV-Visible absorption spectra of PVP-capped CdSe semiconductor nanoparticles at different $CdCl_2$: Se: PVP ratios: A. (1:2:10), B. (1:2:40), C. (1:1:40), D. (2:1:10), E. (2:1:40) and F. (1:1:10).*

The direct band gap in bulk CdSe is 1.74 eV, an absorption peak for CdSe is therefore expected at ~716 nm [40]. Thus, there is a strong blue-shift in the absorption spectra in the as synthesized nanoparticles, indicating that particles must be smaller than the Bohr radius of exciton which is 5.4 nm for CdSe [41]. Figures 4.5 – 4.7 show the TEM micrographs for the CdSe QDs synthesized from the cadmium chloride salt in the presence of PVP. Micrographs for the CdSe nanoparticles synthesized with a mole ratio of Cd: Se: PVP 1:1:20 showed a combination of nanowires with multi-shaped particles dispersed in PVP shown in Figure 4.5A. The thin nanowires were observed and had an

average length of approximately 55 nm. Metallic nanowires have been intensively studied because of the fundamental interests in low-dimensional physics and their technological applications as molecular devices [42,43,44,45]. Long metallic nanowires with well-defined structures and a diameter of several nanometers have been fabricated by using different methods [46,47,48]. Therefore, detailed studies on the structures and properties of such long and nearly free standing ultrathin nanowires are needed. Previous theoretical work include the melting behavior of Pb nanowires [49], nanocrystalline structures of Al and Pb nanowires [50], structural and vibration properties of finite Au nanowires [51], and electronic structures and conductance of Al nanowires [52]. However, the size dependence of atomic structure, vibrational spectra, electronic states, and conductance as well as the structural effect on electronic and transport properties of metallic nanowires are still unclear.

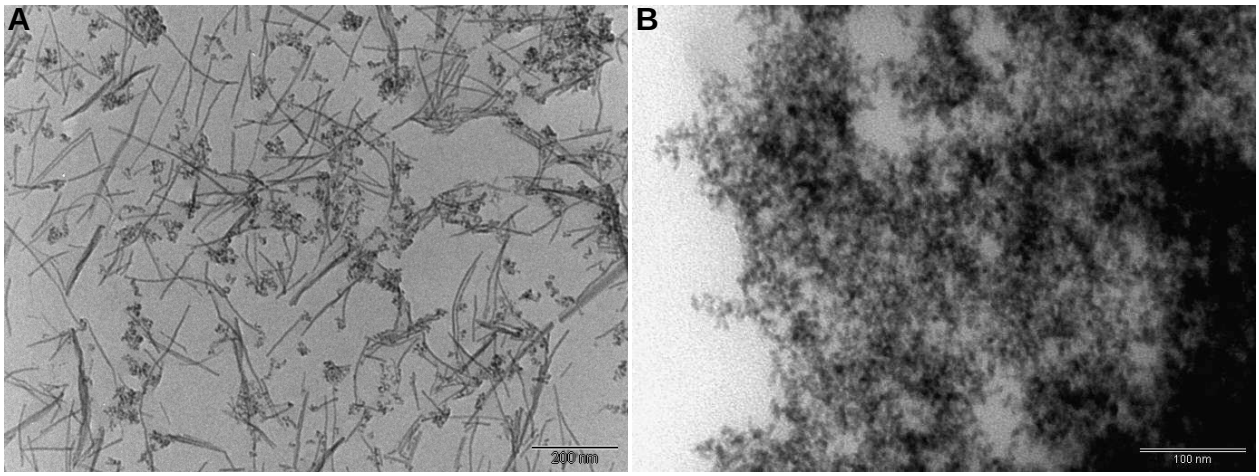

Figure 4.5: *TEM micrographs of PVP-capped CdSe semiconductor nanoparticles at a mole ratio of $CdCl_2$: Se: PVP; A. (1:1:20) and B. (1:1:40).*

Figure 4.5B shows the semiconductor nanoparticles when the PVP concentration (1:1:40) is increased while the other parameters remain constant. The increased capping agent concentration resulted in the formation of the concentrated short rods in solution. The average rod size was about 13.94 nm in length and a width of 2.73 nm. From the structural analysis, further variation of the concentration resulted in the formation of short rods that are well dispersed in the polymer, Figures 4.6 and 4.7. In the same solutions

ordinary shaped particles other than rods were also observed. The average particle size of such nanomaterials is summarized in Table 4.3.

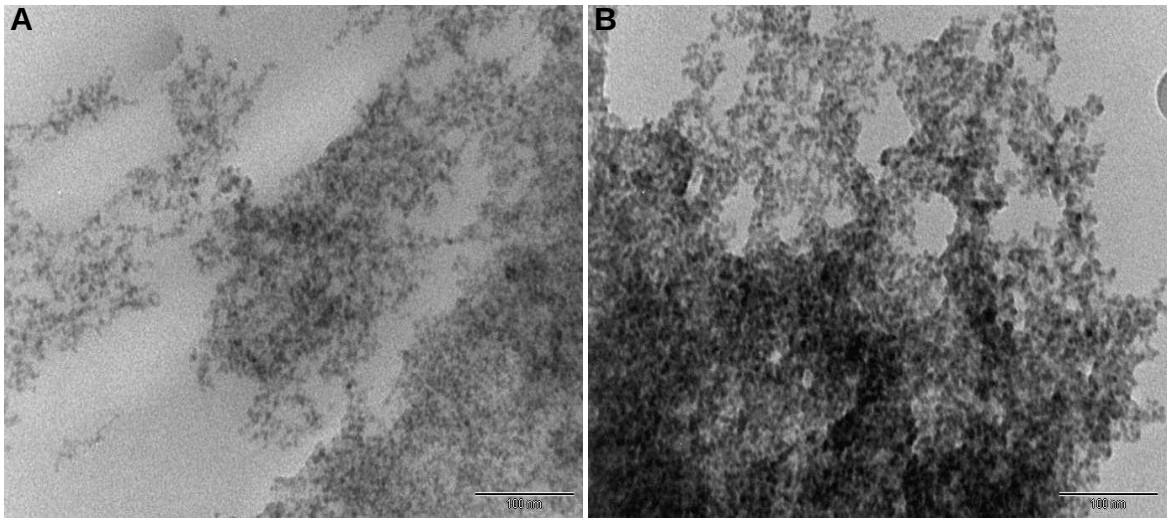

Figure 4.6: *TEM micrographs of PVP-capped CdSe semiconductor nanoparticles at a mole ratio of $CdCl_2$: Se: PVP; A. (1:1:10) and B. (2:1:10).*

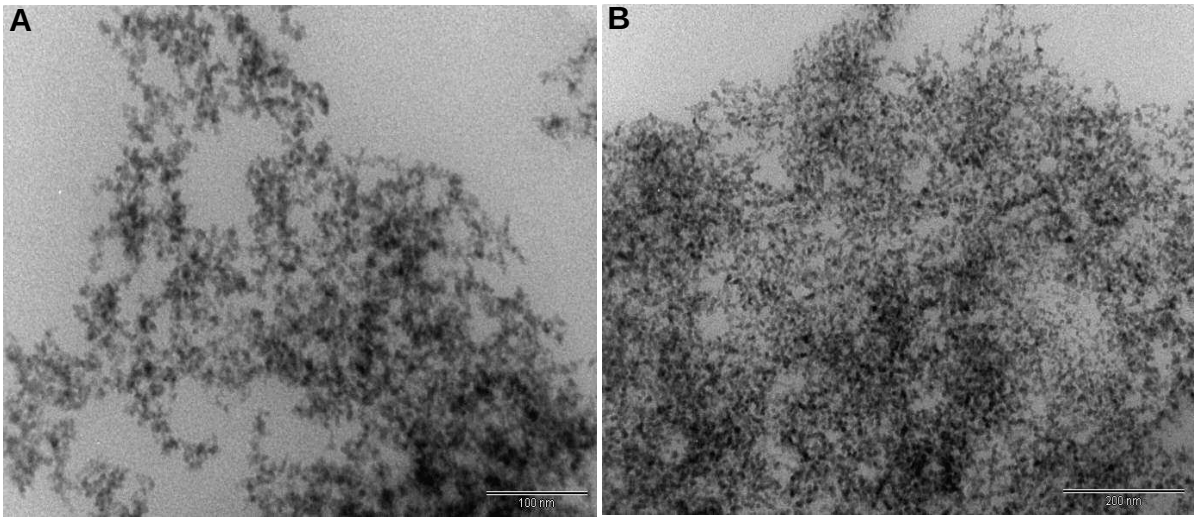

Figure 4.7: *TEM images of PVP-capped CdSe semiconductor nanoparticles at a mole ratio of $CdCl_2$: Se: PVP; A. (1:2:10) and B. (1:2:40).*

Murray *et al.* reported the synthesis of high quality CdSe nanoparticles based on the high-temperature nucleation and growth of nanoparticles from organometallic precursors

[20]. This was done by injecting a solution of dimethylcadmium and selenium in tributylphosphine into a mixture of hexylphosphonic acid (HPA) and trioctylphosphine oxide (TOPO) at 340 – 360 °C [53,54].

Table 4.3: Average particle sizes for the PVP-capped CdSe nanoparticles.

Image / Figure	Average particle size (nm)
4.5 A	6.10 ± 1.46
4.5 B	8.70 ± 1.95
4.6 A	7.92 ± 1.18
4.6 B	11.21 ± 1.67

Alivisatos *et al.* systematically studied the shape evolution of CdSe nanoparticles and various other morphologies, including arrows, pine trees, teardrops, and tetrapods [55]. They further demonstrated that seeded growth of nanocrystals offers a convenient way to design CdSe/CdTe, CdSe/CdS nanoheterostructures with complex shapes and morphologies by changing the crystalline structure of the seed [56].

4.2.2 PVP-Capped Au-CdSe Hybrid Nanoparticles

While possessing uniform and periodic crystal structures, hybrid structures exhibit a very large blue shift in their optical adsorption edge due to strong quantum confinement effects induced by the internal sub-nanostructures [57,58,59]. These compounds exhibit significantly enhanced electronic and optical properties [59,60,61], including a tunable band gap as a result of the strong quantum confinement effect and high band edge absorption [62]. Figure 4.8A shows the absorption spectrum of the Au-CdSe hybrid nanoparticles prepared with the 4.00 x 10^{-3} M gold nanoparticle solution. Significantly, the SPR peak for gold in Au-CdSe metal-semiconductor nanoparticles was broad as compared to that of pure AuNPs solution as inset of Figure 4.8B. Previous reports of hybrid nanocrystals have demonstrated that the optical properties of the colloids are simply a linear combination of the properties of the individual components [63,64]. In the current results the plasmon peak for the sample of AuNPs is located at 540 nm (Figure

4.8A). The plasmon peak of the hybrid Au-CdSe particles is red-shifted by 10 nm compared with the pure AuNPs which absorb at 530 nm. This could be due to the overlap of the electronic states of the different components of the hybrid particles which modifies the surface plasmon resonance [63,65].

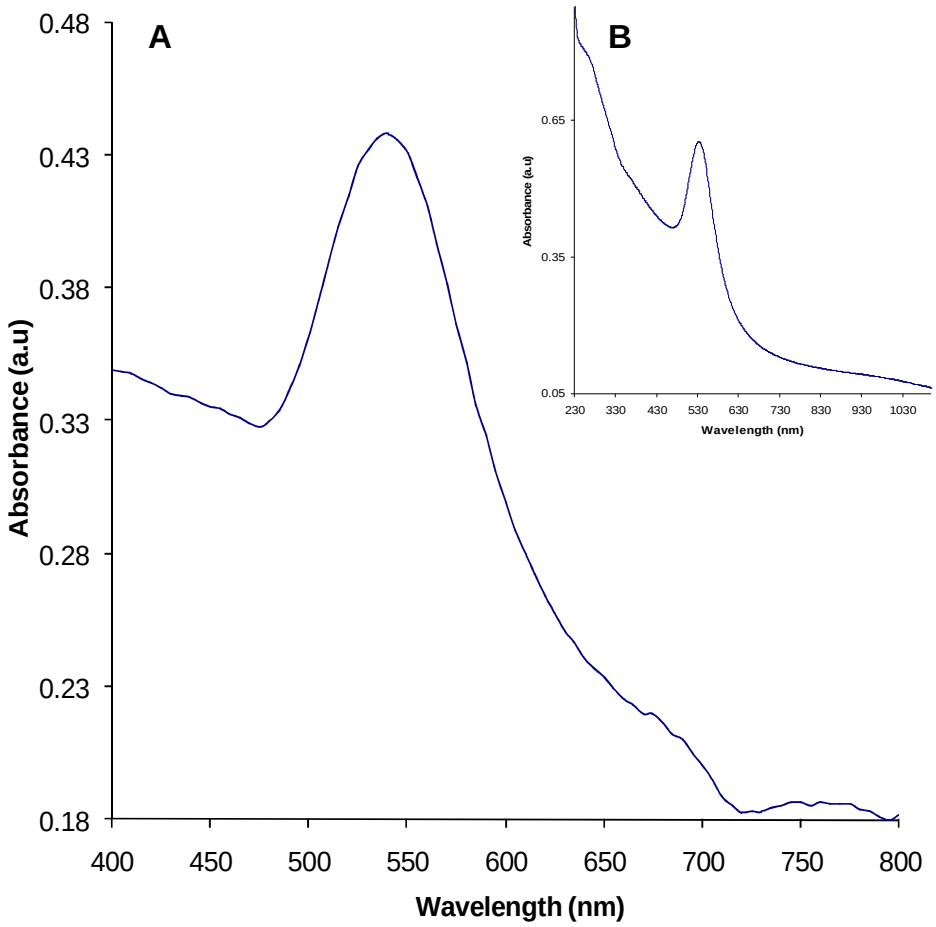

Figure 4.8: *A. UV-Visible absorption spectrum of PVP-Capped Au-CdSe hybrid nanoparticles at 4.00 x 10^{-3} M gold nanoparticle solution. Inset B. UV-Visible absorption spectrum of AuNPs synthesized by UV-irradiation technique light wavelength (450 - 500 nm).*

Alternatively, the shift may reflect that the Au portion of the hybrid nanocrystals is partially covered with CdSe, which possesses the higher index of refraction than the organic capping ligands. The presence of a material with a higher index of reflection is expected to shift the Au plasmon towards longer wavelengths and has been observed

experimentally by varying the reflective index of the solvent [66,67], as well as in hybrid nanocrystals containing Au domains [64]. These Au-CdSe hybrid nanocrystals stabilized by PVP were also analyzed for their structural properties and size using both transmission electron microscopy (TEM) and high resolution TEM. Figures 4.9 and 4.10 shows TEM and HRTEM images of Au-CdSe hybrid nanoparticles respectively.

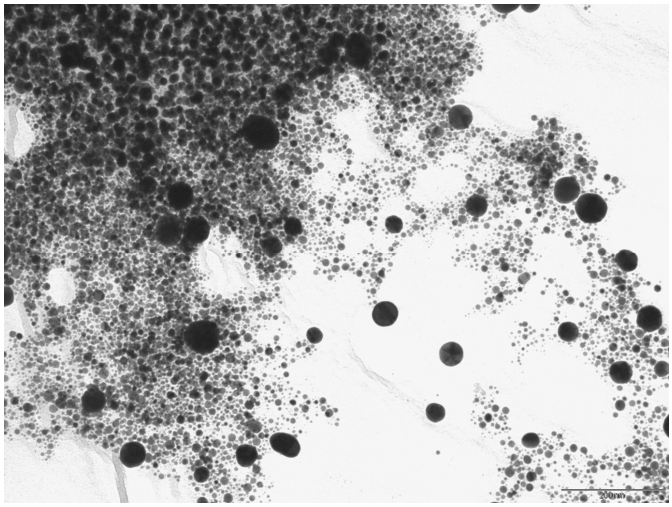

Figure 4.9: *TEM micrograph of PVP-capped Au-CdSe hybrid nanoparticles at Au precursor concentration of 4.00 x 10^{-3} M.*

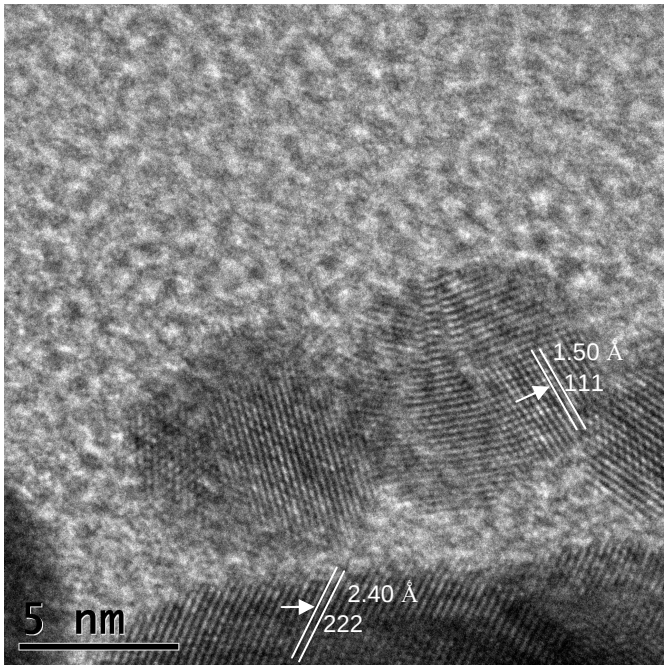

Figure 4.10: *HRTEM micrograph of PVP-capped Au-CdSe hybrid nanoparticles with a Au precursor concentration of 4.00 x 10^{-3} M.*

The TEM micrograph illustrates that the nanomaterials exist as closely packed spherical particles, exhibiting well-defined edges, indicating the composite is composed of individual nanoparticles without evidence of material alloying. The average particle size observed with this precursor concentration was 6.09 ± 1.1 nm. The denser spherical gold particles are distinctly visible in the TEM image. The HRTEM micrograph of these metal-semiconductors shows the presence of lattice fringes at different orientation as seen in Figure 4.10. Such lattice fringes correspond to the gold peaks from the XRD in Figure 4.11. The HRTEM micrograph indicates the crystallinity of the produced hybrid nanocrystal. The lattice spacing of 1.50 Å and 2.40 Å are assigned to the (111) and (222) planes of Au respectively. This is confirmed by X-ray powder diffraction pattern for such nanomaterials as illustrated in Figure 4.11.

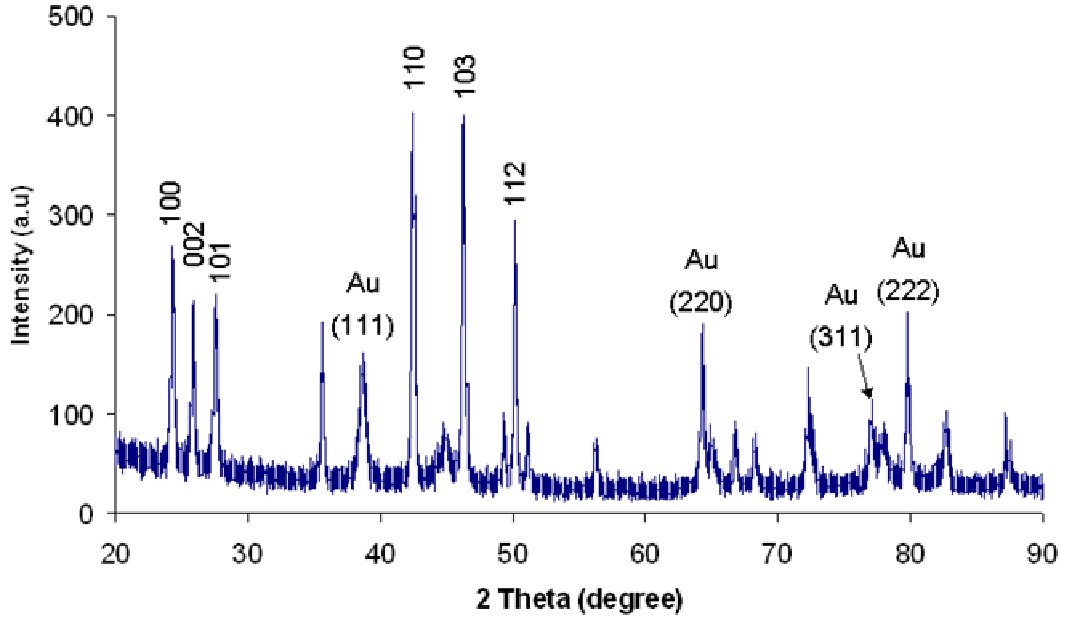

Figure 4.11: *Powder XRD pattern of PVP-capped Au-CdSe hybrid nanoparticles with a Au precursor concentration of 4.00 x 10^{-3} M.*

The peaks (100), (002) and (101) characterize the CdSe nanocrystals and display a hexagonal phase CdSe. This is in agreement with the previous work on the cubic phase CdSe [29]. The (111), (220), (311) and (222) peaks of Au are also observed in the XRD pattern. The XRD data indicate that the Au-CdSe hybrid nanoparticles are of good crystalline quality.

4.2.3 L-Cysteine-Capped Au-CdSe Hybrid Nanoparticles

Au-CdSe hybrid semiconductor nanocrystals capped with L-cysteine were also synthesized and are reported in this section. In this typical experiment, a AuNP stock solution and CdSe nanoparticles capped with cysteine were prepared separately. In the final step, the two solutions were mixed at different concentrations in order to produce Au-CdSe hybrid nanoparticles. Some functional groups, such as cyano (-CN), mercapto (-SH), and amino ($-NH_2$) are known to have high affinity for gold and hence protective polymers having such functional groups are expected to produce AuNPs with a narrow size distribution [68,69]. L-cysteine is a small, zwitterionic molecule, and well used in biochemical and electrochemical research, for an example on a gold surface it has been used to immobilize protein molecules [68]. Figure 4.12 shows the UV-Vis spectrum of cysteine-capped Au-CdSe metal semiconductor nanocrystals. The spectrum shows very little adsorption features. There is a presence of slight shoulder at around 525 nm and no other clear absorption peaks were observed.

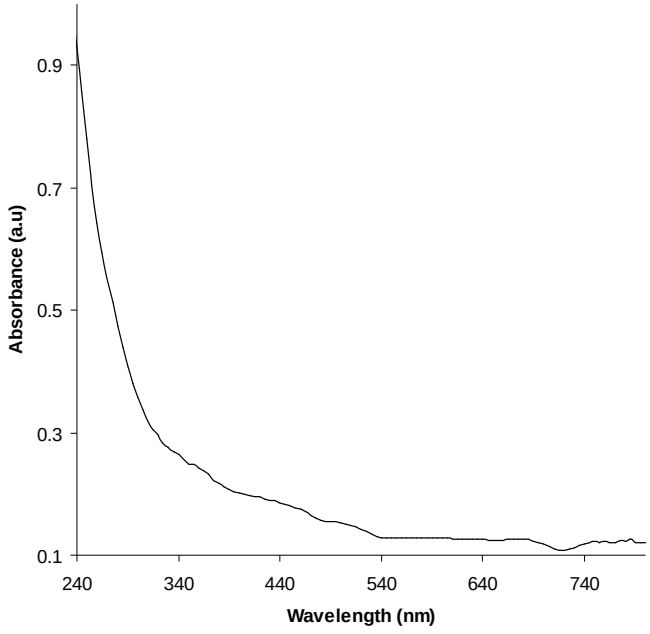

Figure 4.12: *UV-Visible absorption spectrum of L-cysteine-capped Au-CdSe hybrid nanoparticles at 1.60 x 10^{-3} M Au precursor concentration.*

The synthesized Au-CdSe metal semiconductors were further analyzed by TEM for structural information. Figures 4.13 and 4.14 revealed micrographs taken in the presence of 1.60 x 10^{-3} M gold precursor concentration in solution taken at different parts of the copper grid used and the corresponding XRD pattern.

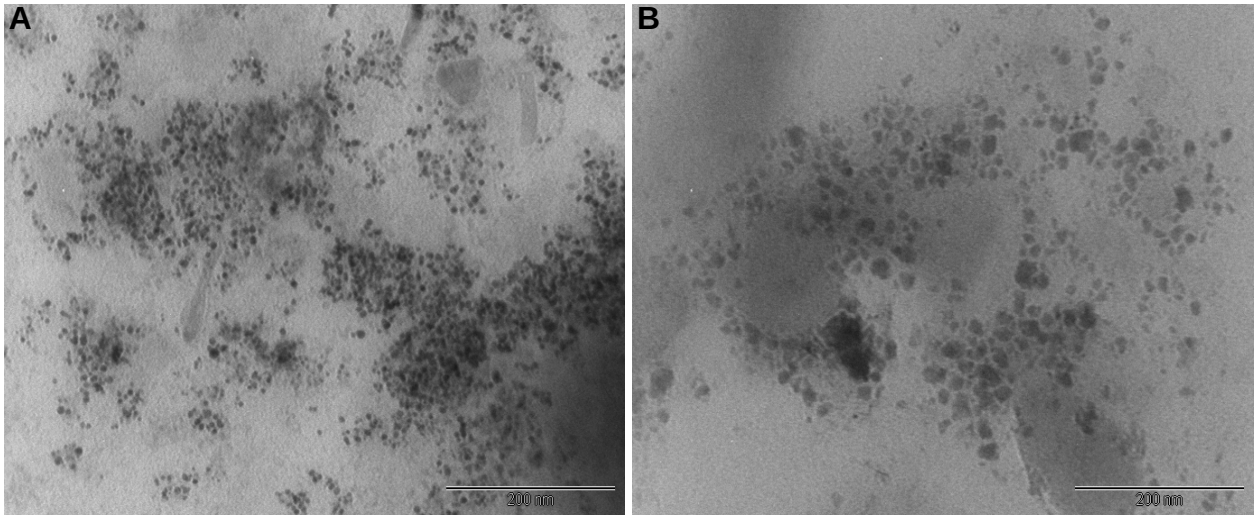

Figure 4.13: *TEM micrographs (A and B) of L-Cysteine-capped Au-CdSe hybrid nanoparticles at Au precursor concentration of 1.60 x 10^{-3} M.*

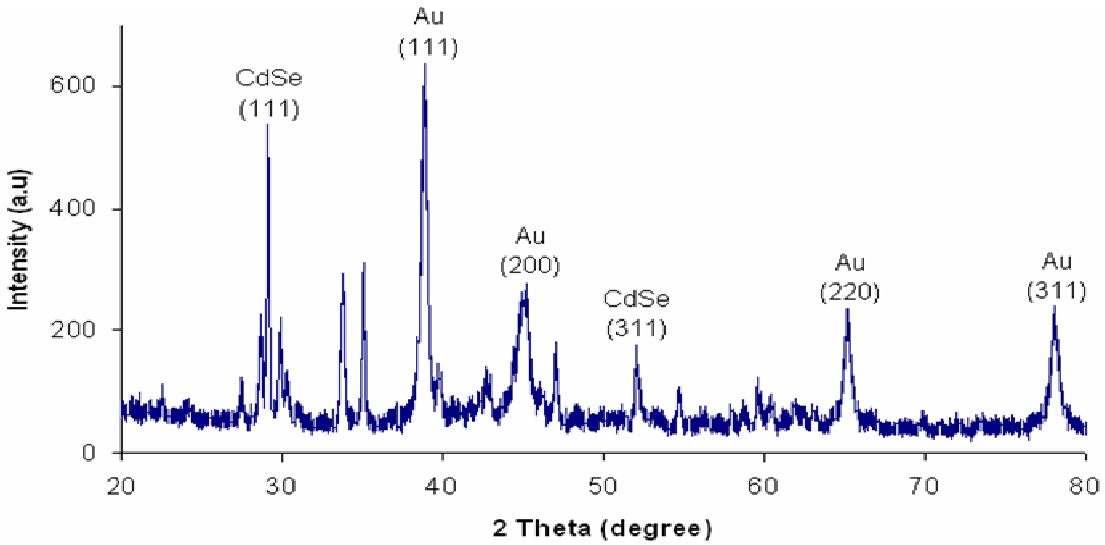

Figure 4.14: *Powder XRD pattern of L-Cysteine-capped Au-CdSe hybrid nanoparticles at Au precursor concentration of 1.60 x 10^{-3} M.*

These images revealed well-dispersed nanoparticles with the presence of shaped-nanocrystals which confirms the presence of the absorption shoulder at longer wavelengths in the UV-Visible spectrum. The hybrid Au-CdSe particles produced at this precursor concentration is reasonably monodispersed showing a combination of morphologies with an average particle size of 9.65 ± 1.74 nm. XRD pattern shows the diffraction peaks that can be indexed to the characteristics of Au and CdSe. The strong (111) peak for both the Au and CdSe is clearly observed in the XRD pattern.

4.2.4 L-Cysteine Capped Gold Nanoparticles

A separate experiment was conducted for the synthesis of AuNPs capped with L-cysteine under UV-light using a column-like mercury lamp (450 – 500 nm) as the reducing agent. In the typical procedure, the Au precursor together with L-cysteine was dissolved in distilled water. The solution was then placed in the UV-reactor and irradiated with UV-light for 1 h with continuous stirring under N_2 atmosphere. The as produced nanoparticles were characterized for their optical and structural properties. From the UV-Visible spectrum, few absorption features were observed for Au as shown in Figure 4.15.

The TEM revealed the presence of gold nanoparticles with varying shapes, but predominantly spherical, ranging from 2 - 14 nm with an average size of 8.29 ± 1.08 nm (Figure 4.16). Particles were widely distributed and were stable in solution for a period of couple of months at room temperature (Figure 4.17). All the diffraction peaks observed in XRD pattern can be indexed to the characteristics of AuNPs. The peaks are assigned to the (111), (200), (220) and (311) diffraction planes of cubic gold respectively. A FT-IR spectrum was employed to detect the characteristic bands of cysteine moiety after gold nanoparticle conjugation. Generally, amino acids are said to exit as zwitterions (internal salts) and exhibit spectral characteristic of both carboxylate and primary amine salts. It shows NH_3^+ stretch which is very broad, N-H bend (asymmetric / symmetric) and COO^- (carboxylate ion) stretch (asymmetric / symmetric) as characteristic vibrations [70,71].

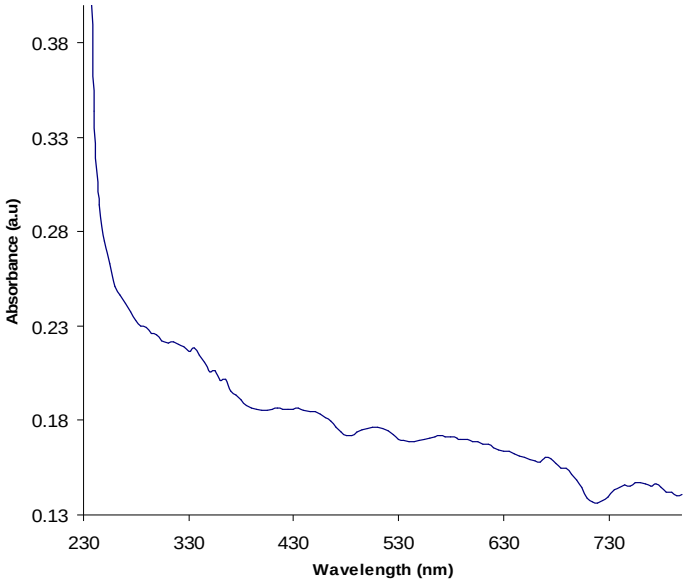

Figure 4.15: *UV-Vis spectrum of L-Cysteine capped AuNPs synthesized under the UV-reactor technique at 1.60 x 10^{-3} M Au precursor concentration.*

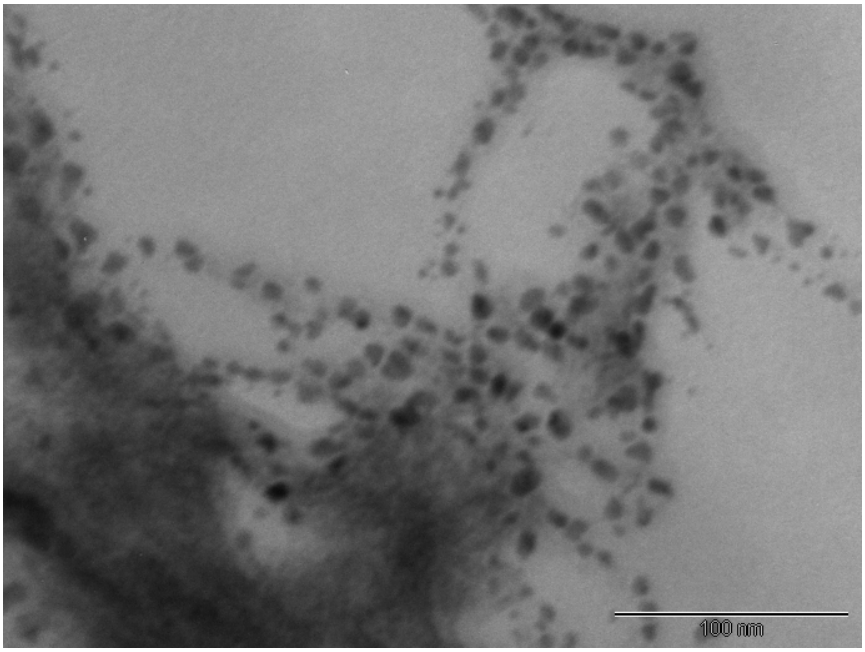

Figure 4.16: *TEM micrograph of L-Cysteine capped AuNPs synthesized under the UV-reactor technique at 1.60 x 10^{-3} M Au precursor concentration.*

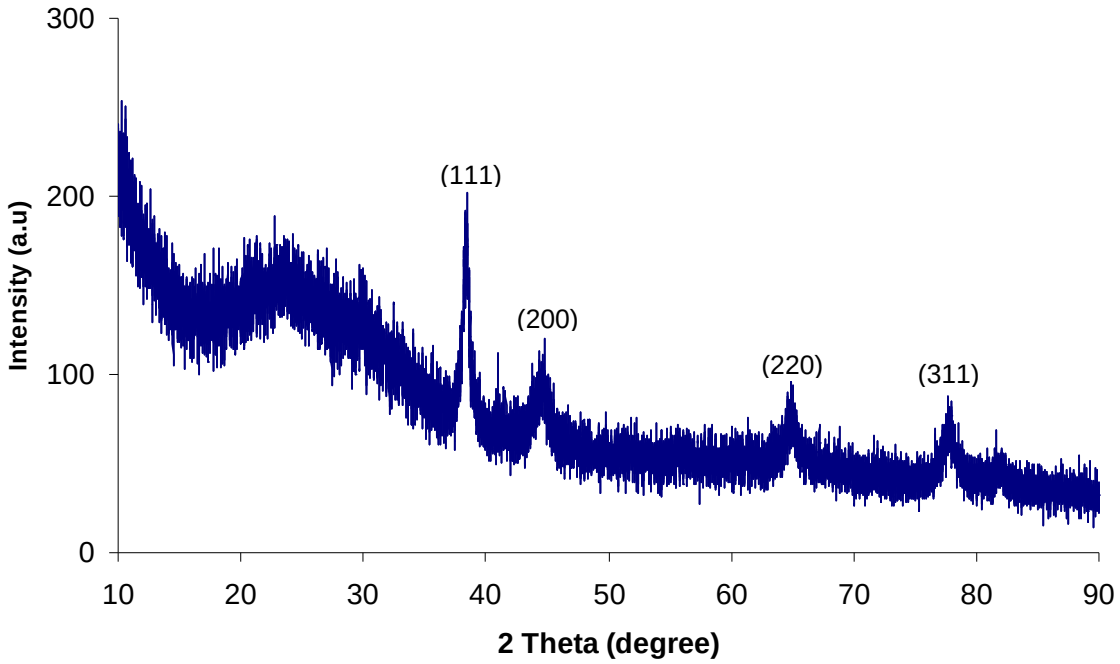

Figure 4.17: *Powder XRD pattern of L-Cysteine capped AuNPs synthesized under the UV-reactor technique at 1.60 x 10^{-3} M Au precursor concentration.*

Figure 4.18 shows the FT-IR spectrum of cysteine capped gold nanoparticles. The band in cysteine at 1600 and 1390 cm^{-1} corresponds to the asymmetric and symmetric stretching of COO^-. A band at 1532 cm^{-1} corresponds to N-H bend and the very broad band of NH_3^+ is observed in the 3000 – 3500 cm^{-1} range. Such results are in good agreement with IR spectra of a typical amino acid. In addition, a weak band near 2550 cm^{-1} virtually confirms the presence of S-H group in the cysteine molecule [70,71]. However slight changes in the reported absorption of cysteine capped gold nanoparticles are observed. A shift in the position of COO^- and NH_3^+ stretching is likely due to a change in their dipole moment when cysteine binds on metal surface with high electron density. Significantly, the band due to S-H was not observed in the spectrum of cysteine capped gold nanoparticles that confirms the S-Au interaction.

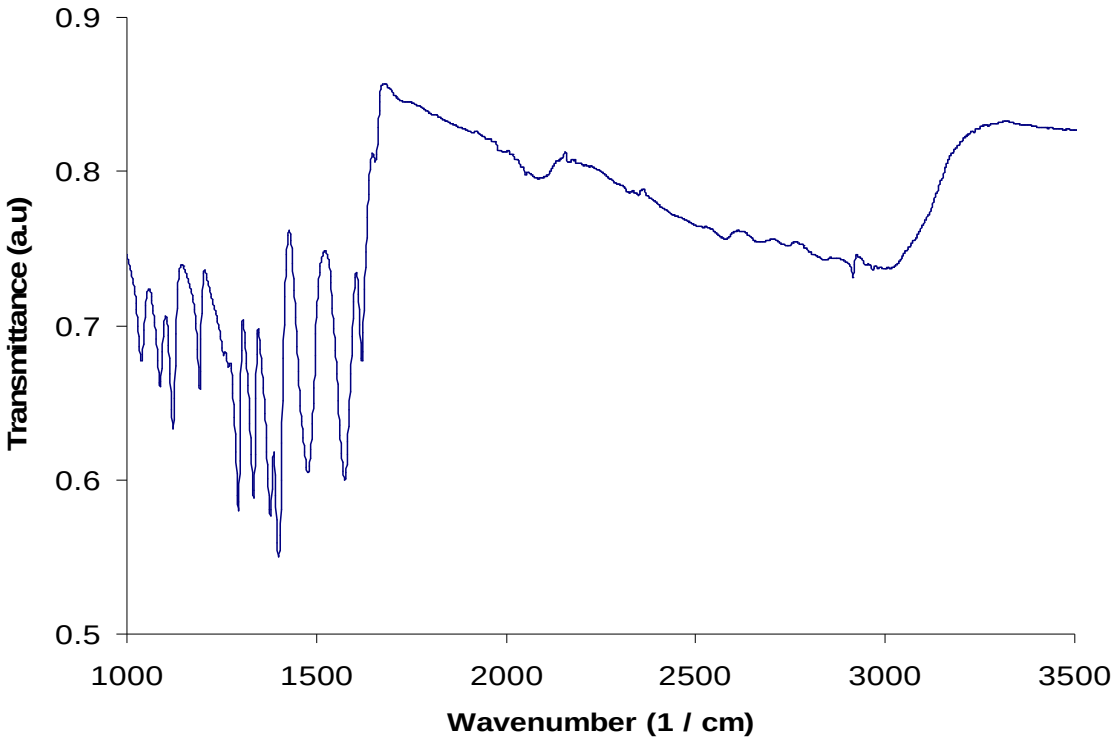

Figure 4.18: *FT-IR spectrum of L-Cysteine capped AuNPs synthesized under the UV-reactor technique at 1.60 x 10^{-3} M Au precursor concentration.*

4.2.5 Synthesis of L-Cysteine-Capped Au-CdSe Hybrid Nanoparticles in the UV-Reactor

L-cysteine capped Au-CdSe hybrid semiconductor nanocrystals were also synthesized under the UV-irradiation technique. In this typical procedure, selenium was reduced in a three necked flask by $NaBH_4$ under N_2 atmosphere for 3 h. The second solution in the UV-irradiation set-up was composed of the precursor $HAuCl_4$ and L-cysteine dissolved in distilled water. The reduced selenium and $CdCO_3$ were simultaneously added to the solution in the UV-reactor. Immediately after this addition the UV-reactor was started in order to reduce the precursor with light and produce the Au-CdSe L-cysteine capped metal semiconductors. The effect of precursor concentration on the synthesized metal semiconductors was studied as outlined in Table 4.2. Figure 4.19 presents the optical properties of hybrid materials taken at different precursor concentrations. These spectra show an absorption shoulder at 255 nm. A broad absorption peak is visible in the long

wavelength range of 530 - 720 nm which could indicate the presence of rods or shaped particles in solution.

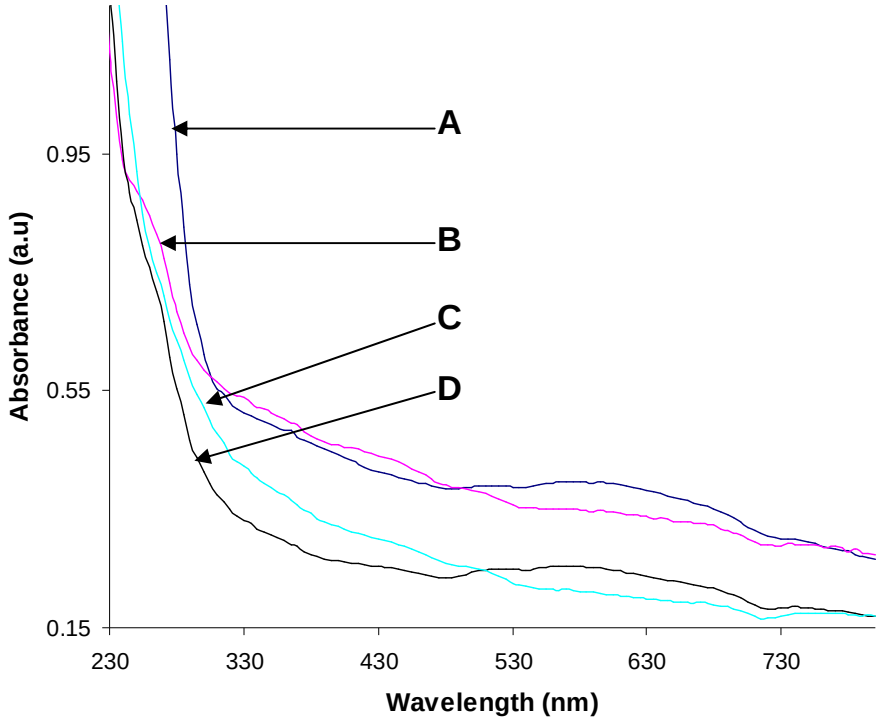

Figure 4.19: *UV-Visible absorption spectra of L-cysteine capped Au-CdSe hybrid nanoparticles at different Au precursor concentration in the UV-reactor: A. (4.00 x 10^{-4} M), B. (8.00 x 10^{-4} M), C. (1.60 x 10^{-3} M) and D. (1.20 x 10^{-3} M).*

Figures 4.20 and 4.21 shows the TEM micrographs of L-cysteine capped Au-CdSe hybrid nanomaterials at different precursor concentrations. Micrograph A in Figure 4.20 shows the morphology of these materials at a lowest precursor concentration of 4.00 x 10^{-4} M to be cloudy due to the higher concentration of capping agent. This cloudy appearance makes it challenging to calculate and measure the particle size. The measured average particle size at this concentration was found to be around 4.64 ± 0.5 nm. As the precursor concentration in solution was increased to 8.00 x 10^{-4} M, clearly visible spherically shaped nanoparticles were observed. The increase in the precursor concentration resulted in an increase in the average particle size to 9.63 ± 1.34 nm, Figure 4.20B.

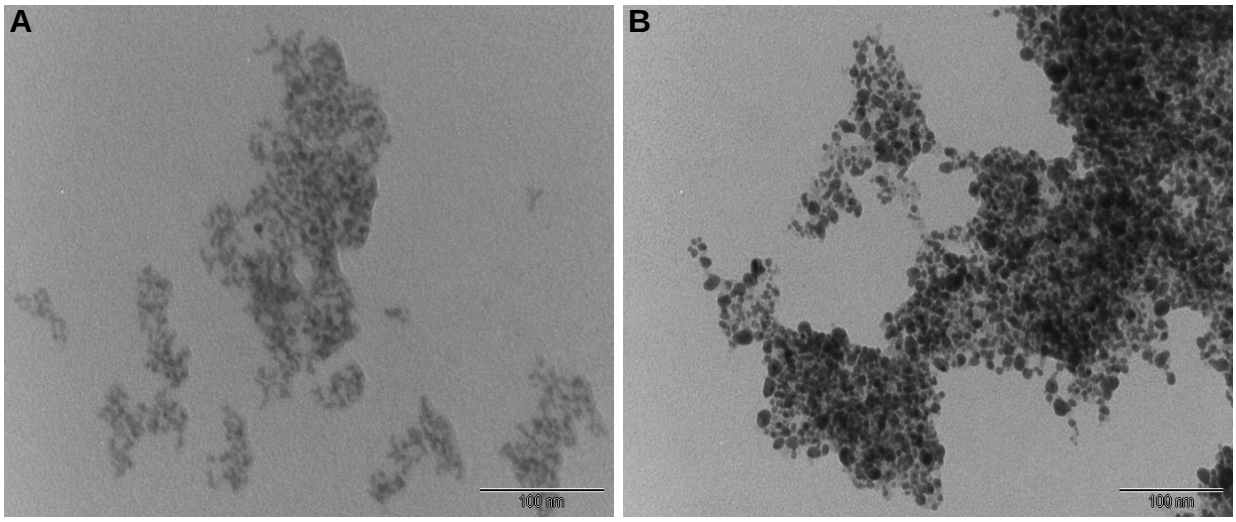

Figure 4.20: *TEM micrographs of L-Cysteine capped Au-CdSe hybrid nanoparticles at Au precursor concentration of A. 4.00 x 10^{-4} M and B. 8.00 x 10^{-4} M.*

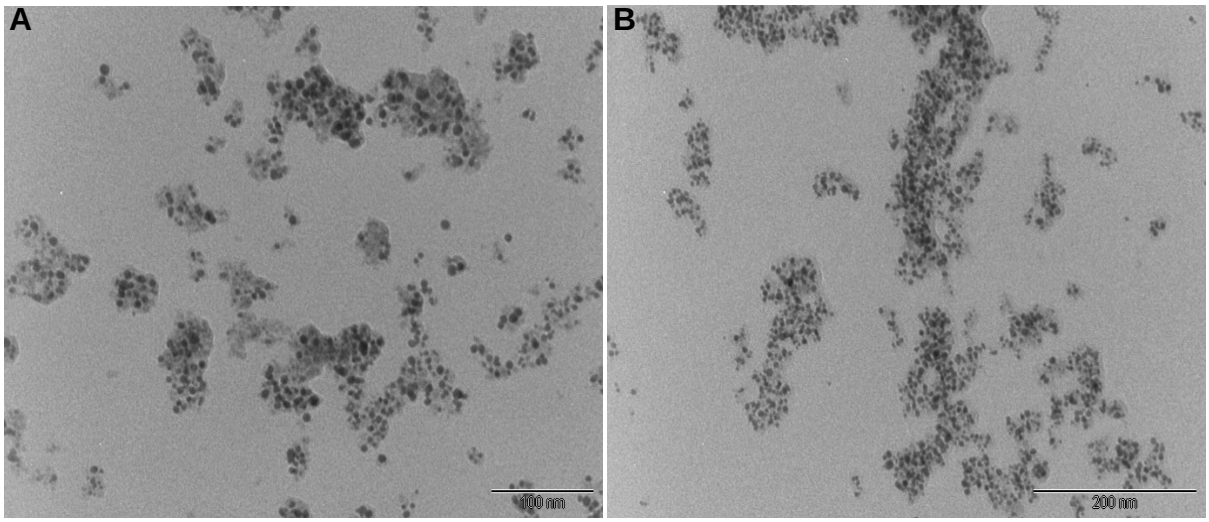

Figure 4.21: *TEM micrographs of L-Cysteine capped Au-CdSe hybrid nanoparticles at Au precursor concentration of A. 1.20 x 10^{-3} M and B. 1.60 x 10^{-3} M.*

A further increase in precursor concentration to 1.20 x 10^{-3} M and 1.60 x 10^{-3} M resulted in well-dispersed metal-semiconductor nanomaterials with an average particle

size of 8.07 ± 1.16 nm and 8.63 ± 1.27 nm as shown in Figure 4.21. In these micrographs the denser Au appearing as dark spots are clearly observed which are surrounded by CdSe semiconductors capped with cysteine. Powder X-ray diffractions measurements were performed in order to characterize the crystal structure of the Au-CdSe nanocrystals as shown in Figure 4.22.

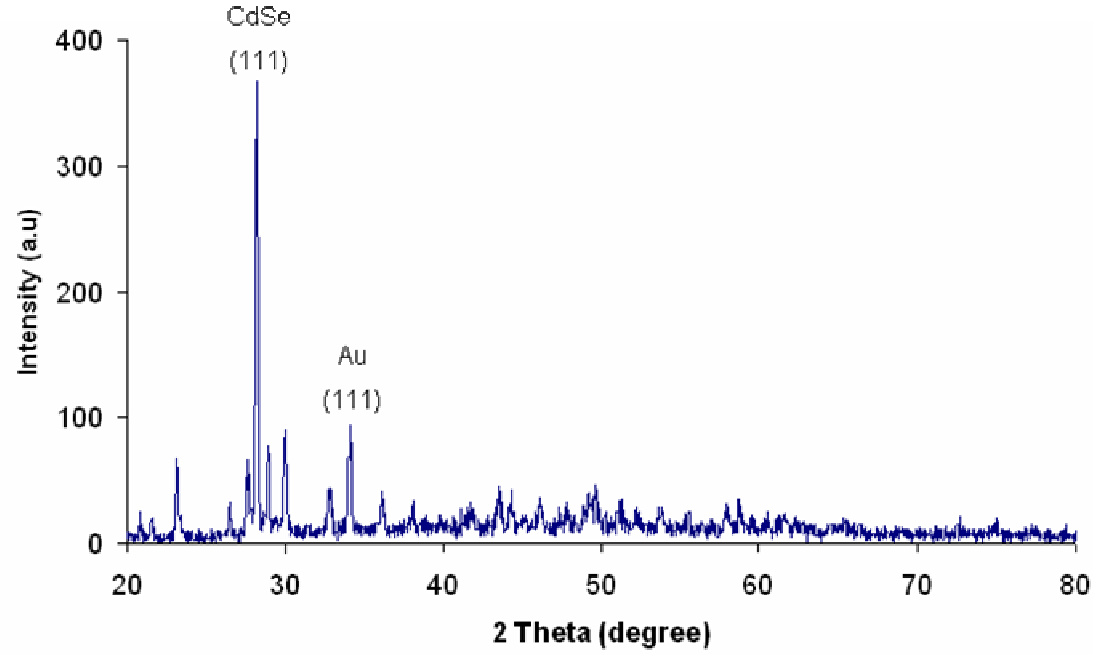

Figure 4.22: *XRD pattern of L-cysteine capped hybrid AuNPs at Au precursor concentration of 4.00 x 10^{-4} M.*

From the XRD pattern, two strong (111) peaks corresponding to CdSe and Au are present. Other peaks at this precursor concentration were suppressed.

4.3 CONCLUSIONS

In this chapter, CdSe semiconductor nanoparticles have been produced at room temperature in the presence of PVP as the capping agent. Different cadmium sources were used and the mole ratio of the starting materials was varied in order to obtain monodispersed CdSe nanoparticles. TEM images showed that $CdCl_2$ is a good source of cadmium as it produced well-defined and dispersed nanoparticles. Plate-like and

nanowires CdSe nanoparticles were obtained as long as 55 nm and nanorods with an average length of 13.94 nm and width of 2.73 nm. From the X-ray diffraction data it is clear that the synthesized CdSe semiconductor nanoparticles are of highly polycrystalline and has hexagonal wurtzite structure. L-cysteine and PVP-capped Au-CdSe hybrid nanostructures have also been synthesized at room temperature. These hybrid nanoparticles display obvious quantum size effect and their optical properties could be fine tuned. The UV-Vis of such materials had showed gold absorption features for the PVP-capped Au-CdSe while for cysteine capped hybrid particles very little features were observed on the spectrum. The structural analysis showed gold as dark spot on TEM images having an average particle size of 6.09 ± 1.1 nm for the PVP capped hybrid nanoparticles and 9.65 ± 1.74 nm for cysteine capped. The high resolution TEM clearly showed the lattice fringes that confirm the crystallinity of the formed PVP capped Au-CdSe hybrid nanoparticles which are also evident from XRD. The XRD data showed strong (111) peak corresponding both to Au and CdSe. The cysteine capped AuNPs showed few absorption features in their optical properties, while the TEM showed the predominance of spherically shaped particles with an average size of 8.28 ± 1.08 nm. These particles were cubic from the XRD data. Further characteristics of these nanoparticles were determined by the FT-IR which showed the stretching bands due to the presence of L-cysteine. Understanding these growth processes and the differences between similar material systems will provide a basis for the rational design of other hybrid nanomaterials and their inclusion into future technologies.

4.4 REFERENCES

[1] X.G. Peng, L. Manna, W.D. Yang, J. Wickham, E. Scher, A. Kadavanich, A.P. Alivisatos, *Nature*, 2000, **404**, 59.

[2] S.H. Kan, T. Mokari, E. Rothenberg, U. Banin, *Nat. Mater.*, 2003, **155**, 2.

[3] L. Manna, D.J. Milliron, A. Meisel, E.C. Scher, A.P. Alivisatos, *Nat. Mater*., 2003, **382**, 2.

[4] R. Jin, Y. Cao, C.A. Mirkin, K.L. Kelly, G.C. Schartz, J.G. Zheng, *Science*, 2001, **1902**, 294.

[5] F. Dumestre, B. Chaudret, C. Amiens, P. Renaud, P. Fejes, *Science*, 2004, **821**, 303.

[6] Z. Tang, N.A. Kotov, M. Giersig, *Science*, 2002, **237**, 297.

[7] J. Goldberger, R.He, Y. Zhang, S. Lee, H. Yan, H.J. Choi, P. Yang, *Nature*, 2003, **599**, 422.

[8] A.Y. Nazzal, L. Qu, X. Peng, M. Xiao, *Nano Lett*., 2003, **3**, 819.

[9] M. Bruchez, M. Moronne, P. Gin, S. Weiss, A.P. Alivisatos, *Science*, 1998, **281**, 2013.

[10] V.L. Colvin, M.C. Schlamp, A.P. Alivisatos, *Nature*, 1994, **370**, 354.

[11] N. Gaponik, I.L. Radtchenko, G.B. Sukhorukov, A.L. Rogach, *Adv. Mater*., 2002, **12**, 879.

[12] L.E. Brus, *Appl. Phys*. A, 1991, **53**, 465.

[13] L. Ouahab, *Chem. Mater.*, 1997, **9**, 1909.

[14] K.E. Andersen, C.Y. Fong, W.E. Peckett, *J. Non-Cryst. Solids*, 2002, **299**, 1105.

[15] J. Lee, V.C. Sundar, J.R. Heine, M.G. Bawendi, K.F. Jensen, *Adv. Mater.*, 2002, **12**, 1102.

[16] Z.A. Peng, X. Peng, *J. Am. Chem. Soc.*, 2001, **123**, 1389.

[17] S.H. Liu, X.F. Qian, J.Y. Yuan, J. Yin, R. He, Z.K. Zhu, *Mater. Res. Bull.*, 2003, **38**, 1359.

[18] S.H. Yu, Y. Yang, Z.H. Han, Y. Zhou, R.Y. Yang, Y.T. Qian, Y.H. Zhang, *J. Mater. Chem.*, 1999, **9**, 1283.

[19] Y. Zhou, L.Y. Hao, Y. Yu, Y.R. Zhu, Z.Y. *Chen, Chem. Lett.*, 2000, **29**, 1308.

[20] C.B. Murray, D.J. Norris, M.G. Bawendi, *J. Am. Chem. Soc.*, 1993, **115**, 8706.

[21] D.V. Talapin, A.L. Rogach, A. Kornowski, M. Haase, H. Weller, *Nano Lett.*, 2001, **1**, 207.

[22] A.L. Rogach, A. Kornowski, M. Gao, A. Eychmuller, H. Weller, *J. Phys. Chem. B*, 1999, **103**, 3065.

[23] L. Han, D. Qin, X. Jiang, Y. Liu, L. Wang, J. Chen, Y. Cao, *Nanotechnology*, 2006, **17**, 4736.

[24] C. Ronny, A.E. Saunders, E. Elmalem, A. Salant, U. Banin, *Nano Lett.*, 2008, **8**, 637.

[25] A.E. Saunders, I. Popov, U. Banin, *J. Phys Chem. B*, 2006, **110**, 25421.

[26] T. Mokari, T. Rothenberg, I. Popov, R. Costi, U. Banin, *Science*, 2004, **304**, 1787.

[27] C. Pacholski, A. Kornowski, H. Weller, *Angew Chem. Int. Ed*, 2004, **43**, 4774.

[28] D.V. Talapin, H. Yu, E.V. Shevchenko, A. Lobo, C.B. Murray, *J. Phys. Chem. C*, 2007, **111**, 14049.

[29] V.S.R. Rajasekhar Pullabhotla, N. Revaprasadu, *Mater. Lett.*, 2009, **63**, 2097.

[30] W.L Shi, H. Zeng, Y. Sahoo, T.Y. Ohulchans, Y. Ding, Z.L. Wang, M. Swihart, P.N. Prasad, *Nano Lett*., 2006, **6**, 875.

[31] M.M. Chili, N. Revaprasadu, *Mater. Lett.*, 2008, **62**, 3896.

[32] S.O. Oluwafemi, N. Revaprasadu, A. Ramirez, *J. Cryst. Growth*, 2008, **310**, 3230.

[33] J.H. Lee, K. Kamada, N. Enomoto, J. Hojo, *J. Colloid and Interface Sc*., 2007, **316**, 887.

[34] Y.T. Lee, S.H. Im, B. Willey, Y. Xia, *Chem. Phys. Lett*., 2005, **411**, 479.

[35] A.R. Roosan, W.C. Carter, *Physica A*, 1998, **261**, 232.

[36] I. Washio, Y.J. Xiong, Y.D. Yin, Y.N. Xia, *Adv. Mater*., 2006, **18**, 1745.

[37] Y. Sun, B. Mayers, T. Herricks, Y. Xia, *Nano Lett.*, 2003, **7**, 955.

[38] Y. Gao, P. Jiang, D.F. Liu, H.J. Yuan, X.Q. Yan, Z.P. Zhou, J.X. Wang, L. Song, L.F. Liu, W.Y. Zhou, G. Wang, C.Y. Wang, S.S. Xie, *J. Phys. Chem. B*, 2004, **108**, 12877.

[39] T. Vossmeyer, L. Katsikas, M. Giersig, I.G. Popovic, K. Diesner, A. Chemseddine, A. Eychmuller, H. Muller, *J. Phys. Chem.*, 1994, **98**, 7665.

[40] A. R. Rogach, A. Korwniwski, M. Gao, A. Eychmuller, H. Weller, *J. Phys. Chem. B*, 1999, **103**, 3065.

[41] S.S. Ashtaputre, A. Deshpande, S. Marathe, M.E. Wankhende, J. Urban, S.K. Kulkarni, *J. Phys*., 2005, **65**, 615.

[42] U. Landman, W.D. Luedtke, N.A. Burnham, R.J. Colton, *Science*, 1990, **248**, 454.

[43] Y. Kondo, K. Takayanagi, *Phys. Rev. Lett*., 1997, **79**, 3455.

[44] W.S. Yun, J. Kim, K.H. Park, J.S. Ha, Y.J. Ko, *J. Vac. Sci. Technol.* A, 2000, **18**, 1329.

[45] Y. Kondo, K. Takayanagi, *Science*, 2000, **289**, 606.

[46] C.J. Muller, J.M. van Ruitenbeek, L.J. de Jongh, *Phys. Rev. Lett.*, 1992, **69**, 140.

[47] U. Landman, W.D. Luedtke, B.E. Salisbury, R.L. Whetten, *Phys. Rev. Lett.*, 1996, **77**, 1362.

[48] H. Hakkinen, R.N. Barnett, U. Landman, *J. Phys. Chem. B*, 1999, **103**, 8814.

[49] O. Gulseren, F. Ercolessi, E. Tosatti, *Phys. Rev. B*, 1995, **51**, 7377.

[50] O. Gulseren, F. Ercolessi, E. Tosatti, *Phys. Rev. Lett.*, 1998, **80**, 3775.

[51] G. Bilalbegovic, *Phys. Rev. B*, 1998, **58**, 15412.

[52] F. Di Tolla, *Surf. Sci*., 2000, **454**, 947.

[53] X.G. Peng, L. Manna, W.D. Yang, J. Wickam, E. Scher, A. Kadavanich, A.P. Alivisatos, *Nature*, 2000, **404**, 59.

[54] L. Manna, E.C. Scher, A.P. Alivisatos, *J. Am. Chem. Soc.*, 2000, **122**, 12700.

[55] D.J. Milliron, S.M. Huhges, Y. Cui, L. Manna, J.B. Li, L.W. Wang, A.P. Alivisatos, *Nature*, 2004, **430**, 190.

[56] D.V. Talapin, J.H. Nelson, E.V. Shevchenko, S. Aloni, B. Sadtler, A.P. Alivisatos, *Nano Lett.*, 2007, **7**, 2951.

[57] S.H. Yu, M. Yoshimura, *Adv. Mater.*, 2002, **14**, 296.

[58] Z.X. Deng, L.B. Li, Y.D. Li, *Inorg. Chem.*, 2003, **42**, 2331.

[59] X.Y. Huang, J. Li, X. Fu, *J. Am. Chem. Soc.*, 2000, **122**, 8789.

[60] C.Y. Moon, G.M. Dalpian, Y. Zhang, S.H. Wei, X.Y. Huang, J. Li, *Chem. Mater.*, 2006, **18**, 2805.

[61] J. Lu, S. Wei, W.C. Yu, Y.T. Qian, *J. Phys. Chem. B*, 2003, **107**, 3427.

[62] Y. Zhang, G.M. Dalpian, B. Fluegel, S.H. Wei, A. Mascarenhas, X.Y. Huang, J. Li, L.W. Wang, *Phys. Rev. Lett.,* 2006, **96**, 026405.

[63] H. Yu, M. Chen, P.M. Rice, S.X. Wang, R.L. White, S.H. Sun, *Nano Lett*., 2005, **5**, 379.

[64] W.L. Shi, H. Zeng, Y. Sahoo, Y. Ding, Z.L. Wang, M. Swihart, P.N. Prasad, *Nano Lett*., 2006, **6**, 875.

[65] D. Steiner, T. Mokari, U. Banin, O. Millo, *Phys. Rev. Lett*., 2005, **95**, 056805.

[66] A.C. Templeton, J.J. Pietron, R.W. Murray, P. Mulvaney, *J. Phys. Chem. B*, 2000, **104**, 564.

[67] K.G. Thomas, J. Zajicek, P.V. Kamat, *Langmuir*, 2002, **18**, 3722.

[68] J. Shan, M. Nuopponen, H. Jiang, E. Kauppinen, H. Tenhu, *Macromolecules*, 2003, **36**, 4526.

[69] T.K. Mandal, M.S. Fleming, D.R. Walt, *Nano Lett*., 2002, **2**, 3.

[70] D.L. Pavia, G.M. Lampman, G.S. Kritz, Introduction to spectroscopy, 3rd Ed., USA, 2001.

[71] A. Pawlukoje, I. Padureanu, D. Aranghel, Inelastic Neutron Scattering, Infrared, Raman Spectroscopy and AB Initio Study of L-cysteine, Report 3 IDRANA 67-04/2004.

CHAPTER FIVE

SUMMARY AND FUTURE WORK

5.0 SUMMARY AND FUTURE WORK

5.1 Summary

The present project resulted in the development of environment friendly methodologies to produce biologically benign gold nanoparticles labeled with biologically and organically relevant molecules. Methods for preparing gold nanoparticles with decreased size, shape dispersity and increased purity are required to ensure that the promise of gold nanoparticles in future technologies is met. In this thesis, several techniques for the synthesis of gold nanoparticles, such as the chemical reduction, seed-mediated method, two-phase method and uv-irradiation technique to synthesize gold nanoparticles were explored. The polymer-protected gold nanoparticles were then expected to have different solubilities in water and in organic solvents. Accordingly, water-soluble particles were obtained, depending on the polymers used in the synthesis. Two kinds of polymers with various molar masses, polyvinylpyrrolidone (PVP), and polyvinyl alcohol (PVA), were chosen for this study and synthesis of gold nanoparticles. Hybrid-gold nanocrystals were synthesized in the presence of either PVP or L-cysteine as capping materials. The optical properties of such materials showed gold absorption features for the PVP-capped Au-CdSe while for cysteine-capped hybrid particles had very little features observed on the spectrum. The structural and crystallographic analysis showed the presence of Au and CdSe.

The synthesis of CdSe semiconductor nanoparticles and Au-CdSe hybrid nanostructures are reported. These semiconductors and hybrid nanostructures were produced at room temperature in the presence of PVP or L-cysteine as capping agents. Understanding these growth processes and the differences between similar material systems will provide a basis for the rational design of other hybrid nanomaterials and their inclusion into future technologies. These semiconductors and gold nanoparticles generated were in the nanometer size range which is deemed realistic for several biological, electronic and catalytic applications.

5.2 Recommendations for Future Work

The knowledge gained from the preliminary experiments done in this project could potentially open new avenues for further research in the development of new synthesis methods for gold nanoparticles with desired properties for various technological and biological applications. The possible pathways to continue the present work are as follows:

1. To use the uv-irradiation technique to synthesize other precious metals such as Pt, Pd which have uses in catalysis.
2. To further study the reaction parameters such as temperature, pH, stirring or not stirring of the solution on the final morphology of the particles.
3. To develop a method of separating particles to achieve a monodispersed shape.
4. To develop a reaction mechanism for the formation of Au nanoparticles from the starting materials.

List of Publications and Presentations

List of Publications and Presentations

1. Synthesis of Anisotropic gold nanoparticles in a water-soluble polymer, **Materials letters**, 62 (2008) 3897.

Conference Presentations

February 2009:	Presented a paper on the NanoAfrica 2009 International conference held in CSIR International Conference Centre, Pretoria.
December 2008:	Presented a paper in SACI International conference held in Cape Town.
October 2008 :	Presented a paper on the 35th International conference of the Southern African Society for Education (SASE)
June –August 2008:	I was an Honorary Staff at the University of Manchester (UK), while doing my PhD research work.
May 2008 :	S.A. PhD Conference.
December 2007:	Attended an International Conference on Materials Chemistry Winter School, Bangalore in India.
October 2007:	Presented a paper on the 34th International conference of the Southern African Society for Education (SASE).
September 2007:	Presented a paper in SACI annual colloquium for KZN institutions.
July 2007 :	International Conference on Materials Research.
Nov. 2006 :	NanoAfrica 2006 2nd Bi-annual Conference by SANI. **Paper Presented**: The synthesis and Characterization of Gold Nanoparticles in water-soluble polymers.
August 2006 :	37th International Conference on Coordination Chemistry. **Paper Presented**: The synthesis and Characterization of Gold nanoparticles in water-soluble polymers.